Two-dimensional near-infrared photonic crystal fabrication by generation of void channels in solid resin

Guangyong Zhou, Michael James Ventura, and Min Gu

Centre for Micro-Phtonics and the Centre for Ultrahigh-Highwidth Devices for Optical Systems, School of Biophysical Sciences and Electrical Engineering, Swinburne University of Technology, PO Box 218, Hawthorn, Victoria 3122, Australia

Received September 29, 2003

Two-dimensional (2D) triangular void channel photonic crystals with different lattice constants stacked in two different directions were fabricated by using femtosecond laser micro-explosion in solid polymer material. Fundamental and higher-order stop gaps were observed both in the infrared transmission and reflection spectra. There is an approximately linear relationship between the gap position and the lattice constant. The suppression of the fundamental gap is as high as 70% for 24-layer structures stacked in the Γ-M direction.

OCIS codes: 230.4000, 160.5470, 300.6340.

Photonic crystals have attracted much interest in recent years after the pioneering suggestion by Yablonovitch[1] and John[2] in 1987 that a photonic bandgap could lead to inhibited spontaneous emission and light localization. Much attention has been devoted to the problem of finding and fabricating three-dimensional (3D) structures that forbid propagation of light in all directions[3−7]. However the fabrication of 3D photonic crystals with bandgap in the near infrared or visible spectral range is still a big challenge. Two dimensional (2D) photonic crystals have also been intensely studied since they are easier to fabricate[8−12], with silicon or other semiconductor lithography being most intensively used. However, the fabrication process is very complicated and realization of high-quality photonic crystals with depth of numerous wavelengths is not trivial. Recently we have developed a new method of fabricating photonic crystals by generating void channels in polymer material by using femtosecond pulsed laser[13,14]. The fabrication is a one-step approach which is carried out within a few tens of minutes using commercially available materials and does not require additional chemical processing. Another advantage of this method is that one can dope functional materials into the polymer to achieve the functionality of devices. 2D triangular structures with different lattice constants were fabricated using this method, and the bandgap properties are reported in this letter.

Figures 1(a) and (b) show the schematic structures used in this work. The first Brillouin zone and irreducible part are shown as the inserts. The light impinges onto the sample from above for both the structure fabrication and the infrared spectral measurements, as indicated by arrows in Fig. 1. For the Γ-M direction, the in-plane spacing is $\delta x = a$, the layer spacing $\delta z = a \cdot \sin 60°$, where a is the lattice constant. For the Γ-O direction, these parameters amount to $\delta x = 2a \cdot \sin 60°$ and $\delta z = a/2$. The experimental setup and blank sample preparation are the same as described in our previous paper except for the objective[13]. The void channels were generated by focusing femtosecond pulsed laser ($\lambda = 540$ nm, repetition rate 76 MHz, pulse width 200 fs, maximum average power 30 mW) into the solid UV-cured Norland NOA63 optical adhesive via a 100×, NA 1.4 oil immersion objective. The ultrashort pulsed laser came from a Ti:sapphire laser with an optical parametric oscillator with an intracavity frequency doubler. The 2D structures were fabricated parallel to the surface of the thin polymer film with the top layer 5 μm below the surface. The size of the fabricated structures was 80 × 80 μm^2. With the exception of $a = 3.0$ μm, all structures consisted of 24 layers of void channels in Γ-M direction and 40 layers of void channels in Γ-O direction, which means that each structure consisted of the same number of void channels. For the structures with the lattice constant $a = 3$ μm, only 20 layers and 34 layers were fabricated for directions Γ-M and Γ-O, respectively, because the laser focus aberrations become very strong if one focuses deeper into the

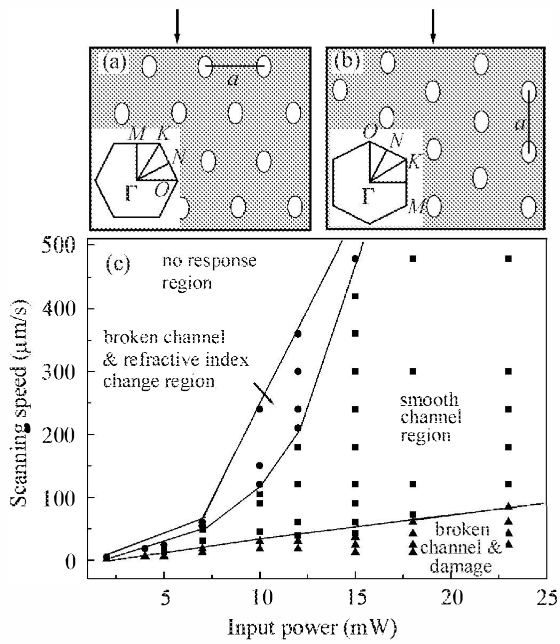

Fig. 1. Sketch of the structure with first Brillouin zone of 2D triangular void channel photonic crystals stacked at Γ-M (a) and Γ-O direction (b) as well as the material response regions with respect to the scan speed and laser intensity (c). The arrows show the incident light direction for both fabrication process and spectral measurement.

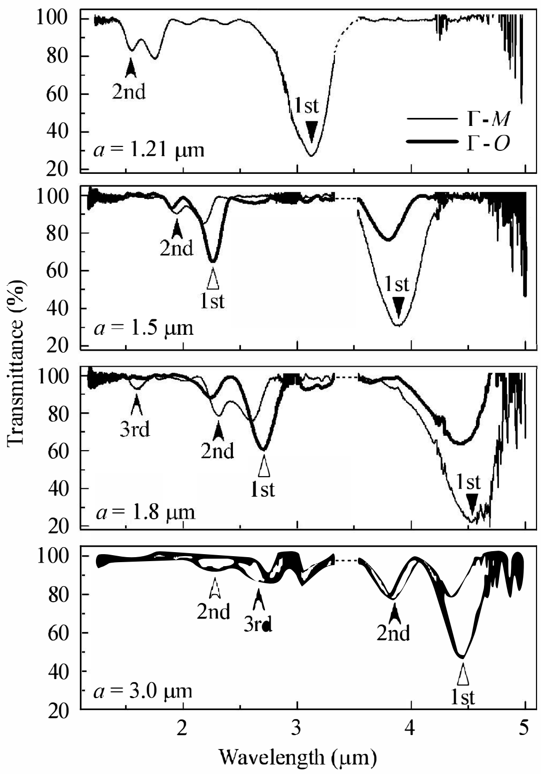

Fig. 2. Infrared transmission spectra of 2D photonic crystals with different lattice constants at directions Γ-M and Γ-O.

sample. Figure 1 (c) shows the material response region with respect to the scan speed and the laser intensity. The data were obtained by examining one single layer of void channels fabricated 20 μm below the polymer surface. It can be seen that smooth void channels can be generated in a large region.

Figure 2 shows the transmission spectra of 2D photonic crystals with different lattice constants at direction Γ-M and direction Γ-O. The fundamental gap was as deep as 70% for all the four lattice constants at direction Γ-M and 40 % at direction Γ-O. High-order gaps can also be recognized in Fig. 2. For the lattice constant $a = 1.21$ μm, the second order gap is located at 1.55 μm, which is a communication wavelength. A NA 0.65 reflective objective was used in the measurement of Fourier transform infrared (FTIR) spectra, which corresponds to 40° maximum incident angle. For this style of FTIR objective, the inner 15° of light cone is blocked. Therefore, this objective provided an incident light cone with the maximum and minimum angle of incidence of 40° and 15°, respectively. Taking into account the refraction at the surface between the cover slip and the air, the corresponding maximum and minimum angle of incidence inside the sample is 10° and 25°. Therefore, the measured results are the average results of different incident angles from 10° to 25°, with the central angle of about 20°.

According to the Bragg scattering theory, the wavelengths of the stop gap and higher-order gaps fulfil the Bragg condition[14]

$$m\lambda_{\text{gap}} = 2n_{\text{avg}}\delta z \cdot \sin\theta, \qquad (1)$$

where m is the order of the gap, n_{avg} is the average refractive index of the photonic crystal, θ is the angle between the incident light and the scattering plane. From the main gap positions and the layer spacing δz, the average refractive index of the photonic crystals can easily be calculated. For the structure stacked along the Γ-M direction with the lattice constant of $a = 1.5$ μm, layer spacing of $\delta z = 1.3$ μm and central wavelength of the fundamental gap of 3.86 μm, the average refractive index n_{avg} was calculated to be 1.58 (assuming $\theta = 20°$).

According to the Bragg scattering condition, the main gaps are located at shorter wavelength for the Γ-K direction than that for the Γ-M direction with the same lattice constant a, which is evident from Fig. 2. Because the cross section of the channels is elliptical with the longer axis along the fabrication laser focusing direction, structures at direction Γ-O with lattice constant $a = 1.21$ μm were not fabricated. From the transmission spectra at direction Γ-M, one can see that the wavelength of the first stop gap at direction Γ-O is shorter than that at Γ-M direction with the same lattice constant.

From Fig. 2 one can see that there are some small stop gaps that do not fulfil the Bragg scattering condition. For example, for $a = 1.5$ μm, there is a stop gap at 2.17 μm at Γ-M direction, just to the right side of the second-order gap at this direction and even deeper than that. Comparing this spectrum with the one for the Γ-O direction, one can easily find that this stop gap just corresponds to the first stop gap in the direction Γ-O. This is caused by the high numerical aperture of the objective used for the measurement of the FTIR transmission spectra, its 10° − 25° range of internal propagation angles generating a large overlap between the two directions, although one direction is still dominating. Consequently, smaller numerical apertures would provide deeper gaps.

Figure 3 shows the relationship between the mid gap wavelength of the gap and the lattice constant at two different stacking directions. The linear relationship is almost for all the gaps, despite the constant channel cross section. Reducing the lattice constant a to 1.085 μm, the main gap of direction Γ-O can be moved to 1.55 μm, which is the optical communication wavelength.

We also observed sharp reflection peaks from the 2D photonic crystals, as indicated in Fig. 4 for the $a = 1.8$ μm structure. The fundamental reflection peaks, second- and third-order peaks can be seen.

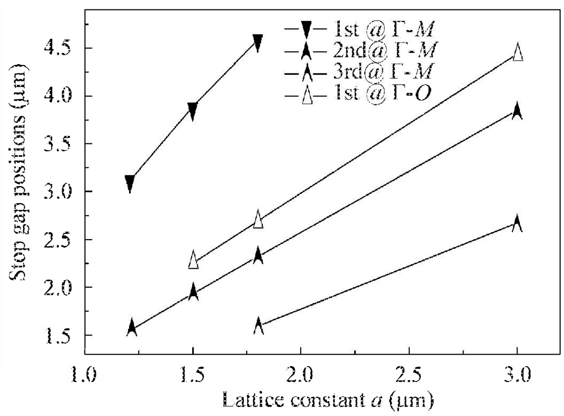

Fig. 3. The relationship of the gap position and lattice constant.

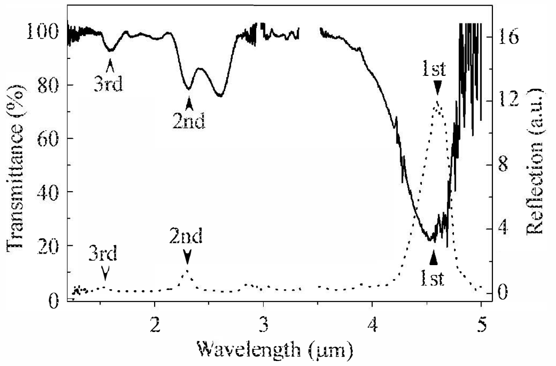

Fig. 4. Reflection and transmission spectra of a 2D triangular void channel photonic crystal with a lattice constant of 1.8 μm.

In conclusion, we fabricated 2D triangular photonic crystals in a commercial resin by femtosecond pulsed laser. The fundamental stop gap suppression can be deeper than 70% at direction Γ-M and 40% at direction Γ-O. The second order stop gap at direction Γ-M is at 1.55 μm, the optical communication wavelength, for the lattice constant $a = 1.21$ μm. Further experiments using smaller channel cross sections are required to move the main gap at directions Γ-M and Γ-O into the telecommunication wavelength region.

This work was produced with the assistance of the Australian Research Council (ARC) under the ARC Centres of Excellence Program. G. Zhou's e-mail address is gzhou@swin.edu.au.

References

1. E. Yablonovitch, Phys. Rev. Lett. **58,** 2059 (1987).
2. S. John, Phys. Rev. Lett. **58,** 2486 (1987).
3. K. M. Ho, C. T. Chan, and C. M. Soukoulis, Phys. Rev. Lett. **65,** 3152 (1990).
4. Z. Y. Li and Z. Q. Zhang, Phys. Rev. B **63,** 1516 (2000).
5. H. S. Sözuer and J. W. Haus, J. Opt. Soc. Am. B **10,** 296 (1993).
6. B. Temelkuran, C. M. Soukoulis, and K. M. Ho, Appl. Phys. A **66,** 363 (1998).
7. S. Y. Lin, J. G. Fleming, D. L. Hetherington, B. K. Simth, T. Biswas, K. M. Ho, M. M. Sigalas, W. Zubrzycki, S. R. Kurtz, and J. Bur, Nature **394,** 251 (1998).
8. T. Zijlstra, E. van der Drift, M. J. A. de Dood, E. Snoeks, and A. Polman, J. Vac. Sci. Tech. B **17,** 2734 (1999).
9. H. Y. Ryu, H. G. Park, and Y. H. Lee, IEEE J. Sel. Top. Quantum Elctron. **8,** 891 (2002).
10. O. Painter, R. K. Lee, A. Scherer, A. Yariv, J. D. O. Brien, P. D. Dapkus, and I. Kim, Science **284,** 1819 (1999).
11. E. Chow, S. Y. Lin, S. G. Hohnson, P. R. Villeneuve, J. D. Hoannopoulos, J. R. Wendt, G. A. Vawter, W. Zubrycki, H. Hou, and A. Alleman, Nature **407,** 983 (2000).
12. N. Kawai, K. Inoue, N. Carlsson, N. Ikeda, Y. Sugimoto, K. Asakawa, and T. Takemori, Phys. Rev. Lett. **86,** 2289 (2001).
13. M. J. Ventura, M. Straub, and M. Gu, Appl. Phys. Lett. **82,** 1649 (2003).
14. M. Straub, M. Ventura, and M. Gu, Phys. Rev. Lett. **91,** 043901 (2003).